ISSN 2706-655X Vol.3, Issue 5: 17-29, DOI: 10.25236/IJFET.2021.030503

Analysis of High Slope Seepage Influence Based on Multi-scale Measurement Data

Yunbo Zhang[1], Haidong Jiang[2]

[1]Guizhou Geological Exploration Institute of General Administration of Sinochem Geological Mine, Guiyang 563100, China
[2]Guizhou Institute of Technology, Guiyang 550081,China

Abstract: *In order to study the influence of seepage on high slope stability, the impact of drainage hole blockage on slope stability is analyzed by in-situ test technology, near-field photogrammetry and indoor test and numerical simulation.According to the groundwater monitoring of the water meter and pore pressure meter, when the drainage hole blockage exceeds 80%, the pore water pressure increases by about 13m, by 25kPa; is monitored by the steel gauge and anchor gauge. When the drainage hole blockage exceeds 80%, the shear force of the slope anti-sliding pile increases by 20%, about 30kN; analyzes the slope deformation by the near-view photography technique, when the drainage hole blockage exceeds 80%, and the slope deformation of 44mm, exceeds the slope deformation warning value of 30mm,.After theoretical calculation and numerical simulation analysis, the groundwater level and support structure under different blockage conditions. Numerical simulation results show that when the drainage hole is less than 60%, the supporting structure and slope deformation grow linearly, while when the blockage degree exceeds 80%, the support structure increases sharply, and according to the finite element strength, when the blockage degree exceeds 60%, the slope stability coefficient decreases sharply and the risk of instability.*

Keywords: *High side slope, In-situ test technology, Near-field photogrammetry technology, Seepage pressure gauge, Rebar dynamometer, Anchor cable axle force gauge, Numerical simulation.*

1. Introduction

Water is one of the key factors causing slope instability, statistical analysis of Genquan (2012) and other scholars[1], more than 88% of foundation pit and slope engineering safety accidents are seepage damage ↔According to the statistics of Yunguichuan and other places, among the geological disasters in mountainous areas, the flood damage disasters have the highest frequency, including the slope section is particularly prominent, and the slope section accounts for about 40%~55% of the whole section [2].

The drain hole is one of the most commonly used ways of slope drainage.After investigation and research, it is found that the drainage pipeline is often blocked due to small particle deposition, groundwater seepage crystallization, microbial growth, etc., thus raising the groundwater level in the slope, which seriously threatens the stability of the slope and the safety of the supporting structure.Therefore, the impact of water volume on the slope stability is the primary engineering geological problem and geotechnical problem solved in the construction of transportation infrastructure in the southwest mountainous area [3].

The stability of the slope caused the attention of some engineers and scholars, Pedescoll and other[4], Hua and other [5], Morvannou and other [6] analyzed the mechanism of artificial wetland blockage and put forward a series of treatment measures.Zhuo Zhou [7] used the model formula to investigate the mechanism of tunnel drainage blockage.Li and other [8], Yanfang Liu and other [9] studied the blockage law of drip pipe under different hardness conditions using drip irrigation test.Richardson, etc. [10], J. Garcia,etc.[11] studies such as Garcia showed that organic deposition, microbial growth and other factors will cause blockage of drainage pipes.The blockage of deep drainage hole on high slope often involves a variety of factors, so it is difficult to study through the above methods. It is an effective auxiliary measure to conduct the coupling analysis of slope seepage field and stress field by numerical method.At present, the mainstream methods of drainage hole simulation are "pipe replacing hole" method [12], wire gathering unit method, drainage substructure method, air unit method etc. In previous studies, the function of the hole; However, the head in the

ISSN 2706-655X Vol.3, Issue 5: 17-29, DOI: 10.25236/IJFET.2021.030503

drainage hole is not equal, and even some zero-head drainage holes, it is not entirely reasonable to simulate the drainage effect by giving the head.According to the principle of head equivalence, the air unit method determines the equivalent permeability coefficient of the drainage hole. And the drainage hole is regarded as a strong penetration medium, simulating the drainage effect. By adjusting the permeability coefficient of the drainage hole, the stress field and seepage field under different blocking conditions of the drainage hole can be calculated.

In order to further obtain the influence of high slope drainage hole blockage on high slope stability, relying on a highway high slope engineering in Guizhou, using in situ test technology, close view photogrammetry technology and numerical simulation analysis, carry out the slope water level change and mechanical response of support structure, quantitatively analyze the impact of drain hole blockage on slope stability.

2. High Groundwater In-situ Test and Data Analysis

In order to study the change of water level in the slope under different working conditions and the mechanical response mechanism of supporting structure, the electronic water level meter, pore pressure gauge, reinforcement stress gauge and the rules of water level and supporting structure, to conduct the slope stability analysis.

2.1. Electronic Water Level Meter and Pore Water Pressure

The blockage of drainage holes, especially under the rainfall conditions, causes the water level of the side slope to rise sharply. By burying the electronic water level meter and hole water pressure meter for the borehole of the high slope project of a expressway in Guizhou, the change of underground water level and water pressure changes during the slope operation period are obtained, see Fig 1&2.

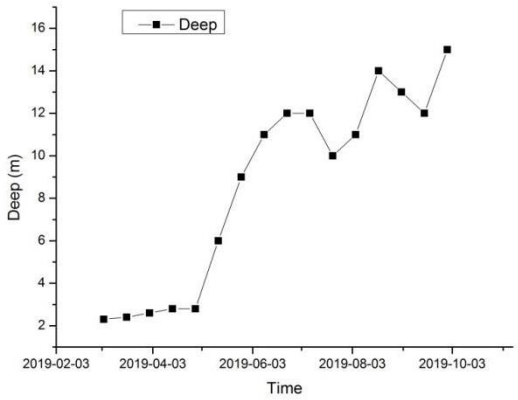

Fig. 1: Statistical diagram of groundwater level change

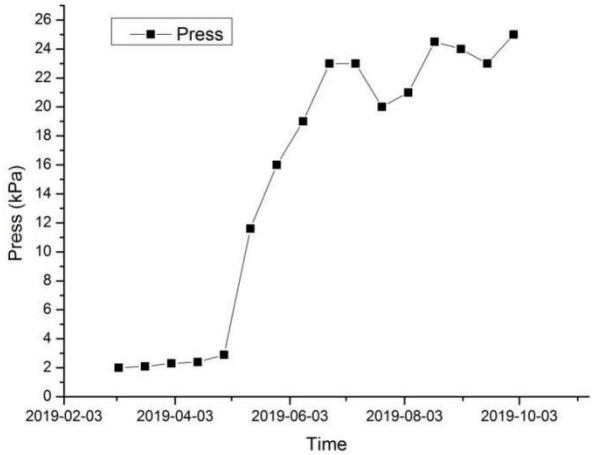

Fig. 2: Monitoring statistics diagram of seepage meter

ISSN 2706-655X Vol.3, Issue 5: 17-29, DOI: 10.25236/IJFET.2021.030503

2.2. Anti-Skid Pile Stress

In the anti-slide pile anchor support structure system, the force of the supporting pile structure is not only affected by the lateral pressure of the soil behind the pile, the passive earth pressure in front of the pile, but also by the tension of the anchor cable and the internal force of the pile itself. In order to study the stress state of the supporting pile at different depths and under different working conditions, the stress state of the supporting pile against soil and by soil side was analyzed by embedding 10 rebar stress meters, see Table 1.

Table 1: Table 1 Parameters of anti-slide pile

R Rebar mm	E Rebar N/mm2	S Rebar mm2	E Concrete N/mm2	S Concrete mm2	E cast-in-place pile N/mm2	S mm2	Fy	kN
28	1.95*105	15393.8	2.8*104	7.7*105	31371.2	7.85*105	360	221.67

Note: Rebar type HRB400, Concrete type C30

By testing the force of the main reinforcement of the supporting pile, the forces on the side of the soil facing and facing face of the cast-in-place pile structure are calculated back, see Fig 3. According to the principle of deformation coordination, the calculation principle is based on the calculated strain of rebar = rebar strain = concrete pile strain:

$$\varepsilon_g = \sigma_g / \mathrm{E}_g \tag{1}$$

In the formula: ε_g is rebar strain, σ_g is rebar stress, E_g is the elastic modulus of rebar.

$$\varepsilon_z = \sigma_z / \mathrm{E}_z \tag{2}$$

In the formula: ε_z is the strain of the cast-in-place pile, σ_z is the stress of the cast-in-place pile and E_z is the elastic modulus of the cast-in-place pile.

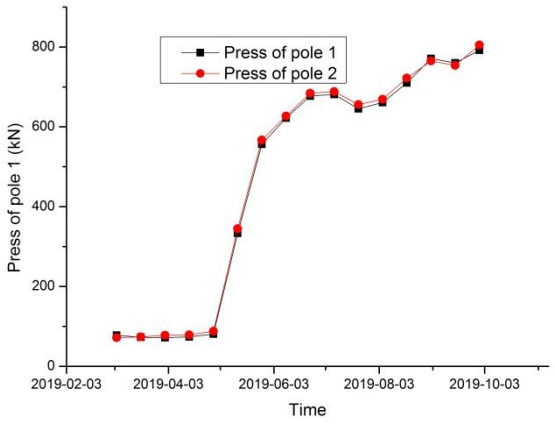

Fig. 3: Statistical chart of rebar stress gauge monitoring data

2.3. Force of Anchor Cable

The prestressed anchor cable is transferred to the soil around the anchor through the cable strand and the cohesive force of the mortar, thus providing the anchoring force for the mortar.

$$\Delta L = \frac{PL}{EsAs} \tag{3}$$

In the formula: ΔL is the elongation of the anchor cable (mm), P is the tensile force (N), L is the length of the free section of the prestressed anchor cable (mm), Es is the elastic modulus of the anchor

ISSN 2706-655X Vol.3, Issue 5: 17-29, DOI: 10.25236/IJFET.2021.030503

cable (2×105N/mm2), and As is the total cross-sectional area of the steel strand in each hole (mm2).

In order to study the stress state of the supporting pile at different depths and under different working conditions, the stress state of the anchor cable was analyzed by embedding two anchor cable axial force meters (See Fig.4).

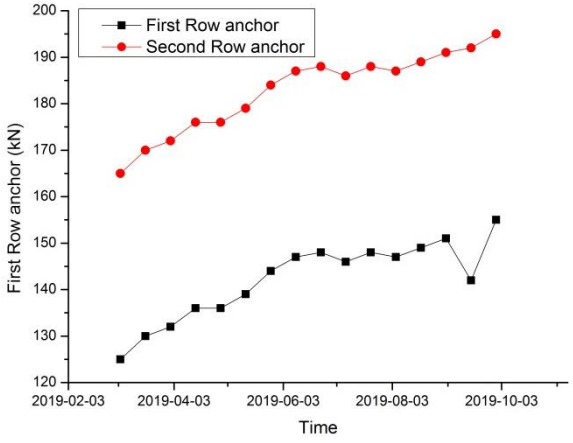

Fig. 4: Statistical chart of cable axial force meter monitoring data

2.4. Data Analysis

After an annual monitoring and statistical analysis of hydrology, when the blockage degree of drainage holes exceeds 80%, the groundwater is monitored by water level gauge and pore permeability gauge, and the groundwater level of the slope rises about 13m, and the pore water pressure increases by 25kPa. The shear force of the main reinforcement of the slope anti-slide pile increases by 20%, and the axial force of the anchor cable increases by about 30kN through the monitoring of the steel bar meter and the anchor cable axial force meter.

3. Non-Contact Digital Near-Field Photogrammetry Technology

3.1. Technical Principle of Non-Contact Digital Near-Field Photogrammetry

Non-contact digital near-field photogrammetry technology is to calculate the spatial three-dimensional coordinates of the target point on the basis of the image information of the target point and the relevant parameters of the digital camera, using the optical principle and the spatially known target.Suppose a point $P(X,Y,Z)$ in space whose projection points on two photos are $P'(x_1,y_1)$ and $P''(x_2,y_2)$ respectively.The camera taking the photo is located in the projection center$S(X_s,Y_s,Z_s)$, and the three angles between the coordinate system and the P point are ω,φ,k, and the focal length of the camera is f. P、P'（orP''）and S three points are on a straight line and, depending on the collinear equation, the relationship between the three can be expressed by the following formula.

$$x_i = -f\cdot\frac{r_{11}(X-X_s)+r_{12}(Y-Y_s)+r_{13}(Z-Z_s)}{r_{31}(X-X_s)+r_{32}(Y-Y_s)+r_{33}(Z-Z_s)} \tag{4}$$

$$y_i = -f\cdot\frac{r_{21}(X-X_s)+r_{22}(Y-Y_s)+r_{23}(Z-Z_s)}{r_{31}(X-X_s)+r_{32}(Y-Y_s)+r_{33}(Z-Z_s)} \tag{5}$$

In the formula, $i=1,2,r_{ij}$ can be represented by the following relation, that is:

$$R(\omega_i,\ \varphi_i,k_i)=R(\omega_i)R(\varphi_i)R(k_i)=\begin{bmatrix}r_{11} & r_{12} & r_{13}\\ r_{21} & r_{22} & r_{23}\\ r_{31} & r_{32} & r_{33}\end{bmatrix} \tag{6}$$

and

$$R(\omega_i)=\begin{bmatrix}1 & 0 & 0\\ 0 & \cos\omega_i & \sin\omega_i\\ 0 & -\sin\omega_i & \cos\omega_i\end{bmatrix}$$

ISSN 2706-655X Vol.3, Issue 5: 17-29, DOI: 10.25236/IJFET.2021.030503

$$R(\varphi_i) = \begin{bmatrix} \cos\varphi_i & 0 & -\sin\varphi_i \\ 0 & 1 & 0 \\ \sin\varphi_i & 0 & \cos\varphi_i \end{bmatrix}$$

$$R(k_i) = \begin{bmatrix} \cos k_i & \sin k_i & 0 \\ -\sin k_i & \cos k_i & 0 \\ 0 & 0 & 1 \end{bmatrix}$$

Of course, the three-dimensional coordinates of the space point P can not be determined based on the spatial point alone, and in order to further solve them, another set of relations needs to be established.It can be found from the figure that P is in the same plane as the two camera points S' and S'' in two different locations, so you can establish a coplanar equation of the three, i. e.:

$$F = \begin{vmatrix} b_x & b_y & b_z \\ u_1 & v_1 & w_1 \\ u_2 & v_2 & w_2 \end{vmatrix} = 0 \tag{7}$$

Among them

$$\begin{bmatrix} u_i \\ v_i \\ w_i \end{bmatrix} = \begin{bmatrix} 1 & -k_i & -\varphi_i \\ k_i & 1 & -\omega_i \\ \varphi_i & \omega_i & 1 \end{bmatrix} \begin{bmatrix} x_i \\ y_i \\ -f \end{bmatrix} \quad i = 1, 2$$

In the formula, $\begin{bmatrix} b_x \\ b_y \\ b_z \end{bmatrix}$ is the vector size between points $S'$and S''.

3.2. Analysis of the Deformation Measurement Data

Based on the feasibility, advantage and disadvantages of the technology,, PhotoModeler Scanner from Eos is used as photogrammetry processing and analysis software, and Panasonic FZ-35 and Canon Eos 7D are used as image acquisition tools.

Non-contact near-field photography on high slope of an expressway in Guizhou, the measurement results are Figure 5:

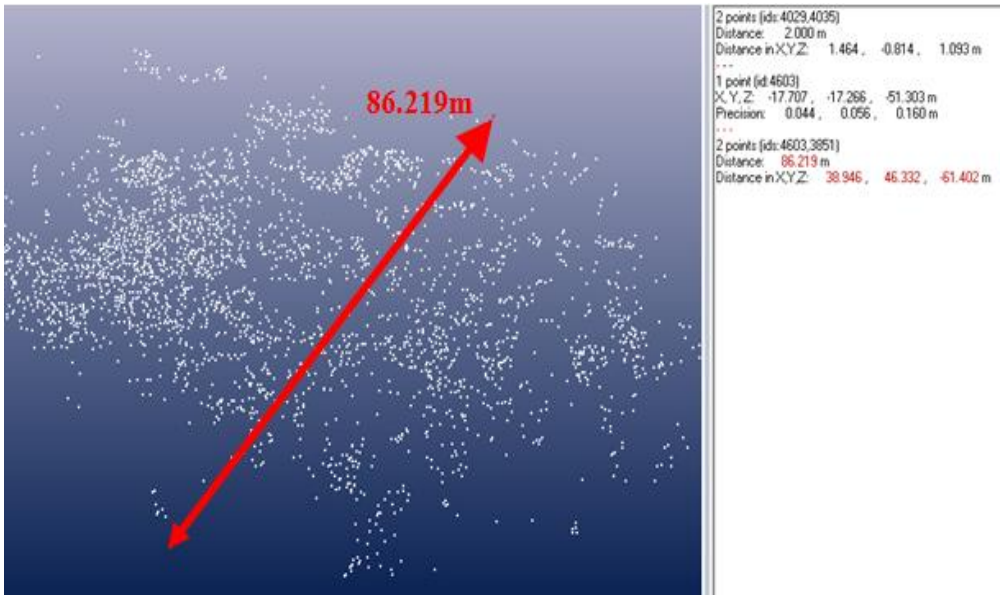

Fig. 5: Three dimensional coordinates and distance of any scatter

According to the statistical analysis, the drainage hole of an expressway slope in Guizhou province is more than 80% blocked, and the maximum displacement is 39.78mm, which is 30mm more than the alarm value of slope deformation, and the risk of slope instability exists.

ISSN 2706-655X Vol.3, Issue 5: 17-29, DOI: 10.25236/IJFET.2021.030503

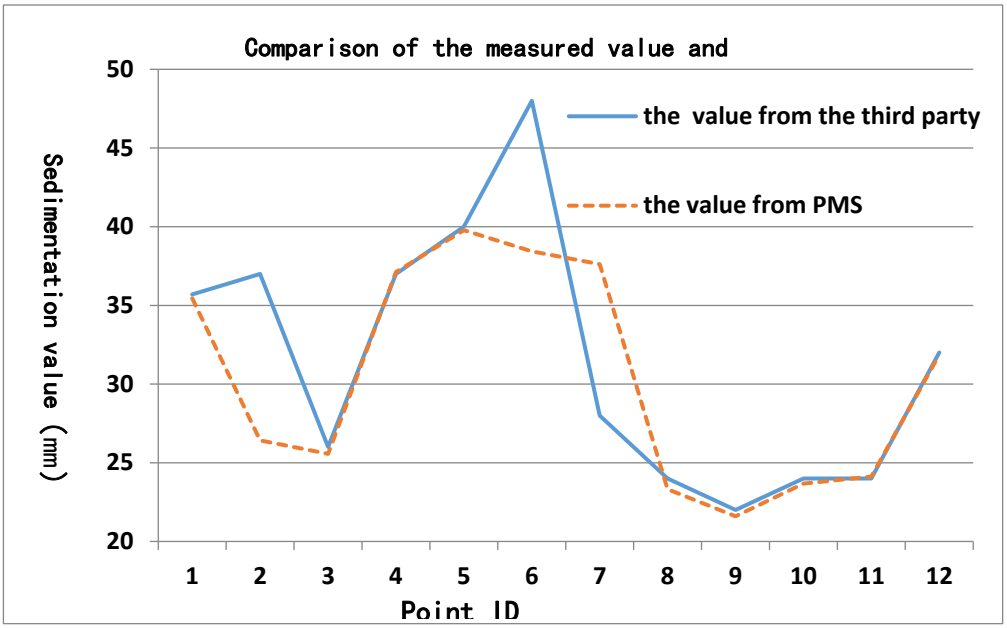

Fig. 6: Statistical analysis diagram of the slope displacement point

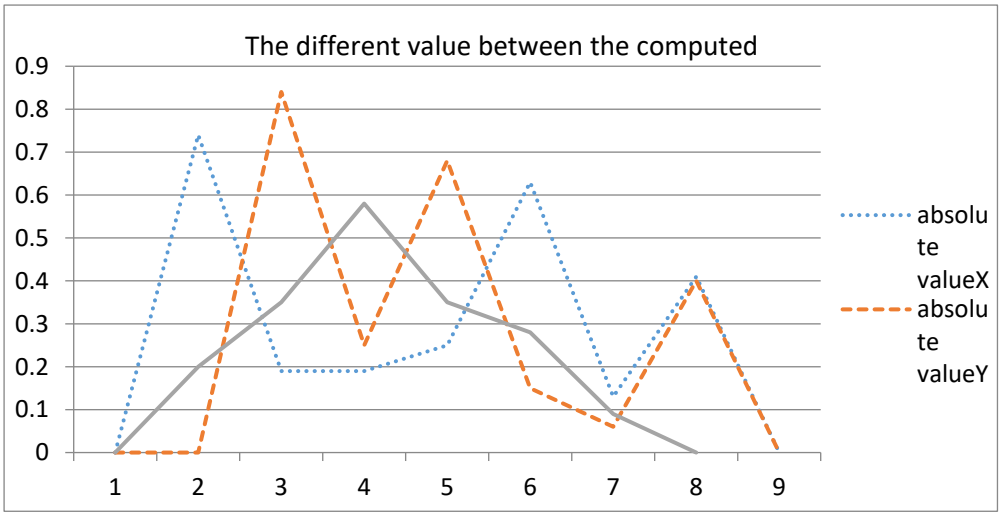

Fig. 7: Statistical analysis diagram of measurement data error

After analysis from Fig.6&7, non-contact near-field photogrammetry technology is adopted, and the displacement measurement error in each direction is less than 1mm, and the accuracy meets the technical requirements.

4. Numerical Calculation and Simulation

4.1. Prototype Parameters and Constitutive Model

The rock layer of a slope project of Guizhou Expressway is divided into two layers, the first layer is silty clay and about 1 m; thick, the second layer is slightly weathered limestone.The slope is supported by two ways, one is lattice anchor block wall and the other is pile anchor support system.

Three-dimensional model of retaining wall slope extension direction: 6 m, overall model size is 100 m(long) × 6 m(wide) 77 m(high), rock body and drainage hole adopt C3D8RP hole pressure unit, C3D8R three-dimensional stress unit, and T3D2 embedded truss unit.The 3-dimensional model for numerical calculation of anchor pull pile slope is shown in Figure 10. With the anti-skid pile, the slope extension 60 m, 30 m, slope extension is 6 m, model size is 112 m(long) × 6 m(width) 77m(high).C3D8RP hole pressure unit is adopted for rock body and drainage hole, C3D8R 3-dimensional stress unit for skid pile and concrete retaining wall and T3D2 embedded truss unit for

ISSN 2706-655X Vol.3, Issue 5: 17-29, DOI: 10.25236/IJFET.2021.030503

anchor cable.

4.2. Calculate the Parameters and the Boundary Conditions

The calculation parameters of ABAQUS numerical simulation conditions are shown in Table 2.

Table 2: Model Parameters

Material	Material model	Density (kg/m3)	Elastic modulus (GPa)	The Poisson ratio	Sated penetration coefficient (m/s)	Bonforce (MPa)	Friction angle (°)
Rock mass	Mohr.Coulomb	2450	0.9	0.35	4.75E-7	4.168	35.23
Drainage holes	Linear elastic	1.0	0.9	0.35	4.75E-1	-	-
Drainage plate	Linear elastic	2480	0.9	0.35	3.56E-5	0.28	30
lattice Configur-ation	Drucker.Prager	2550	28	0.3	-	-	-
Anchor rod	Linear elastic	7800	210	0.2	-	-	-
Anti-skid pile	Drucker.Prager	2550	28	0.3	-	-	-
Ananchor cable	Linear elastic	7800	210	0.2	-	-	-

4.3. Simulation of Working Condition

According to the groundwater level monitoring data and the permeability coefficient of the rock and soil body on the indoor test slope is 0.475 m/s, the drainage plate is used to replace the drainage hole for ABAQUS numerical simulation calculation based on Table 3.

Table 3: Calculation and working conditions

Working condition	Saturated permeability coefficient of the drainage hole	Blocking degree	Working condition	Saturated permeability coefficient of the drainage hole	Blocking degree
Working condition11	4.75×10-1	Normal drainage	Working condition 4	4.75×10-5	Blockage 60%
Working condition2	4.75×10-3	Blockage 20%	Working condition 5	4.75×10-6	Blockage 80%
Working condition3	4.75×10-4	Blockage 40%	Working condition 6	4.75×10-7	Blockage 100%

5. Numerical Calculation Results and Measurement Data Analysis

5.1. Comparative Analysis of the Groundwater Level Changes

Through numerical simulation, the saturation of slope rock mass under different working conditions is obtained. Figure 8 shows the cloud map of slope saturation change of lattice anchor bar, and Figure 9shows the cloud map of slope saturation change of anchor pull pile.The red part in the figure represents that the rock mass reaches full saturation, the orange part is basically saturated, the blue part

ISSN 2706-655X Vol.3, Issue 5: 17-29, DOI: 10.25236/IJFET.2021.030503

is the lowest, and the saturation of the rock mass also reflects the change of the groundwater level to some extent.

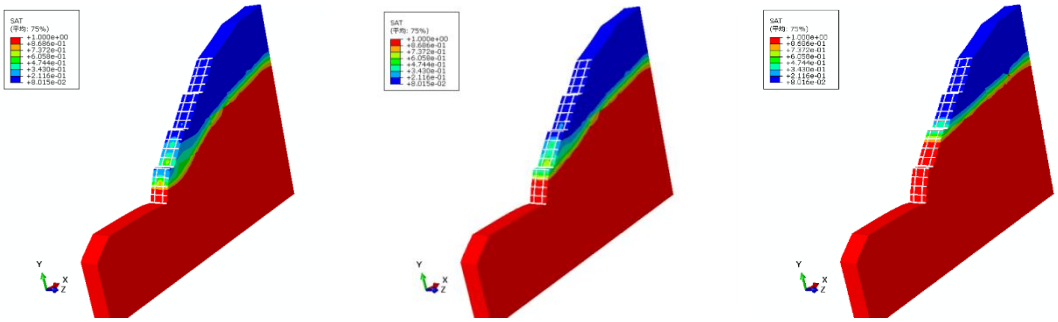

(a) Normal drainage (b) Blockage 20% (c) Blockage 40%

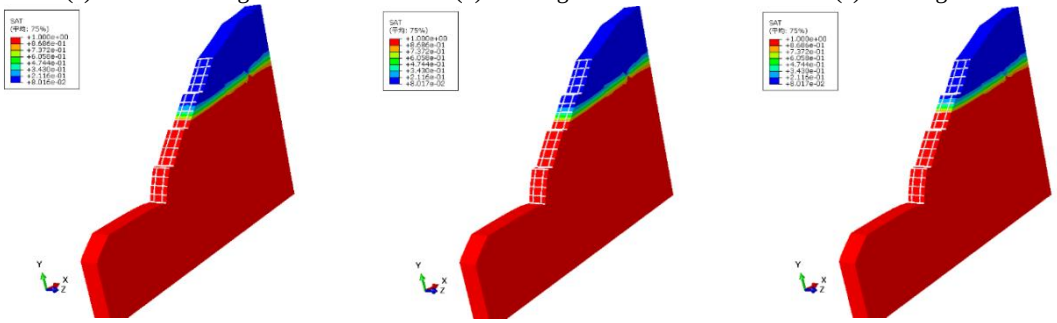

（d）Blockage 60% (e) Blockage 80% (f) Blockage 100%

Fig. 8 Cloud chart of saturation change of lattice anchor retaining wall slope

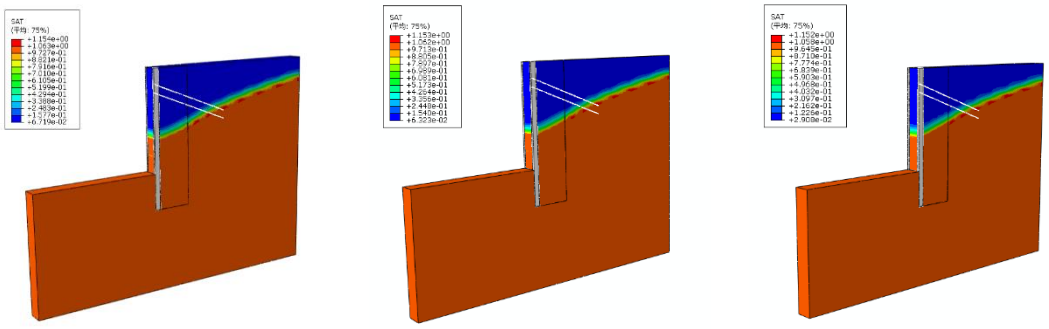

(a) Normal drainage (b) Blockage 20% (c) Blockage 40%

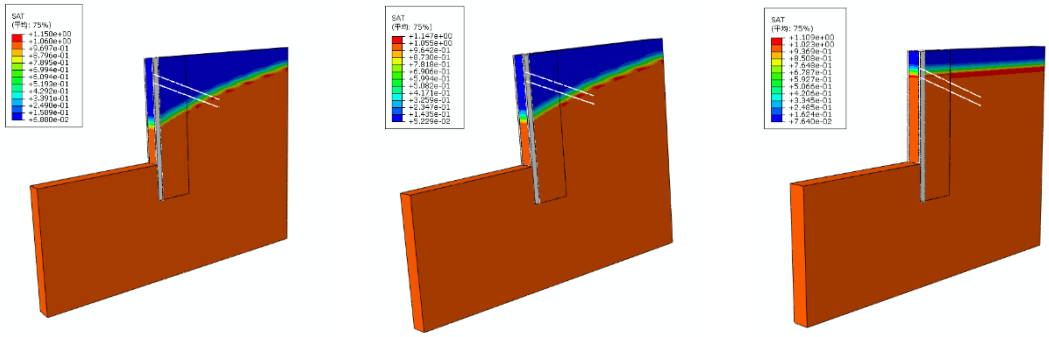

(d) Blockage 60% (e) Blockage 80% (f) Blockage 100%

Fig. 9: Cloud chart of saturation change of anchored pile slope

Through mathematical simulation and comparative analysis of measurement data from Fig.8&9:

(1) Under the form of lattice anchor rod support, when the blockage degree is 40%, the groundwater level rises nearly 10 meters compared with 20%; when the blockage degree exceeds 60%, the groundwater level rises relatively slowly.

(2) Under the form of anchor pull pile support, the groundwater level increases slowly with the blockage degree. After the blockage degree exceeds 80%, the blockage level is less than 40%, the

ISSN 2706-655X Vol.3, Issue 5: 17-29, DOI: 10.25236/IJFET.2021.030503

groundwater level change range is not large, and the groundwater level rise is less than 1 m. When the drainage hole is completely blocked, the groundwater level reaches 13.8 meters, and the lifting range is nearly twice the blockage of 80%.

5.2. Comparative Force analysis of the Support Structure

The destruction of slope is the process of deformation and overrun of stress field.Side slope stability is studied by analyzing the stress state of the support results, and the numerical simulation results are shown in Figure 10-13:

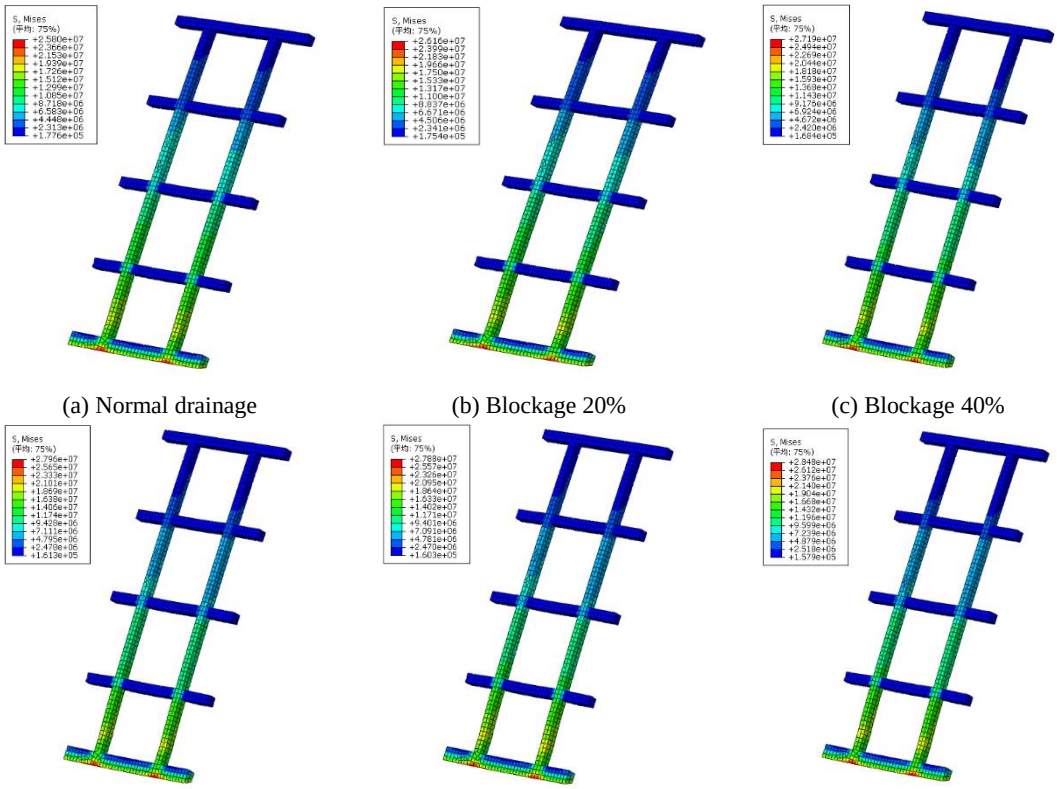

(a) Normal drainage (b) Blockage 20% (c) Blockage 40%

(d) Blockage 60% (e) Blockage 80% (f) Blockage 100%

Fig. 10: Lattice stress cloud chart

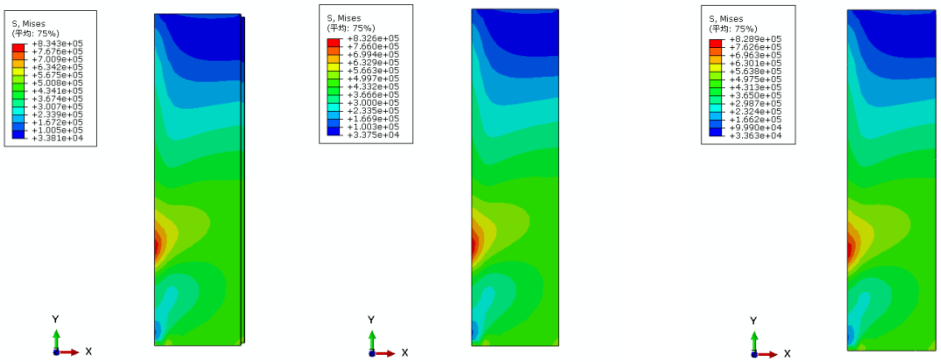

(a) Normal drainage (b)Blockage 20% (c)Blockage 40%

ISSN 2706-655X Vol.3, Issue 5: 17-29, DOI: 10.25236/IJFET.2021.030503

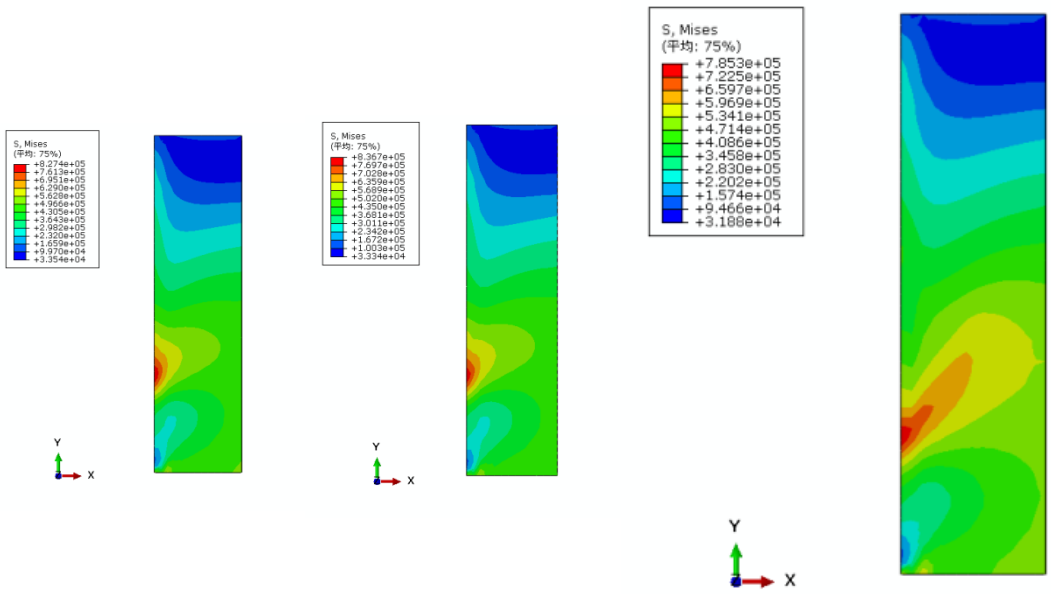

(d)Blockage 60% (e)Blockage 80% (f)Blockage 100%

Fig.11: Stress chart of anti-slide pile

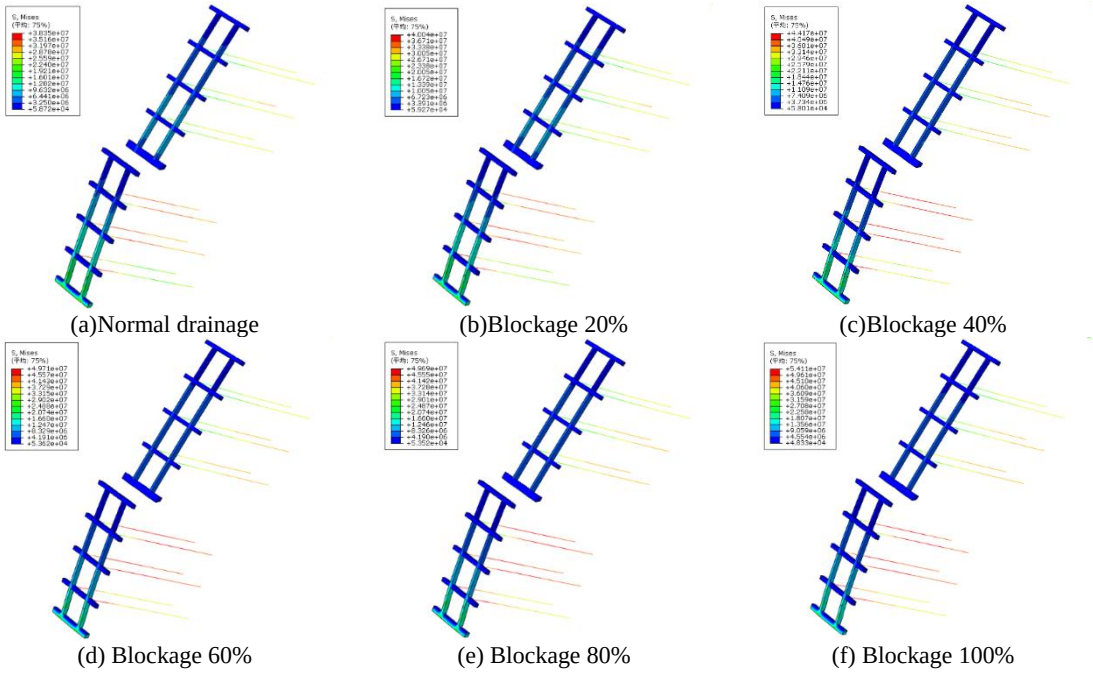

(a)Normal drainage (b)Blockage 20% (c)Blockage 40%

(d) Blockage 60% (e) Blockage 80% (f) Blockage 100%

Fig. 12: Axial force cloud chart of anchor rod

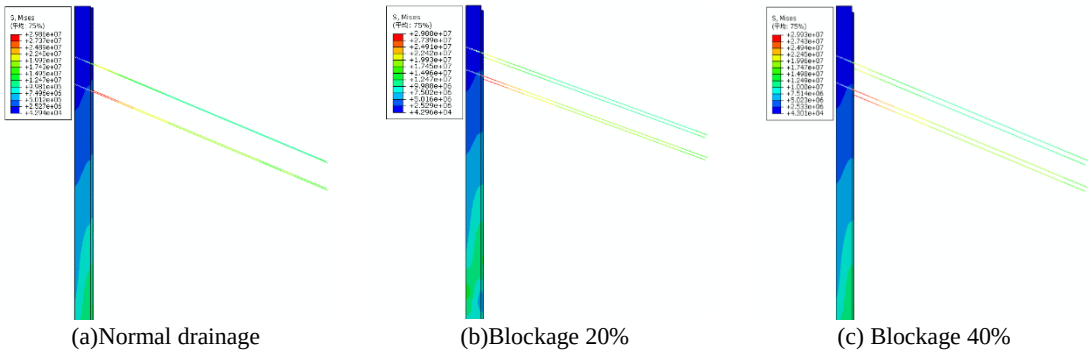

(a)Normal drainage (b)Blockage 20% (c) Blockage 40%

ISSN 2706-655X Vol.3, Issue 5: 17-29, DOI: 10.25236/IJFET.2021.030503

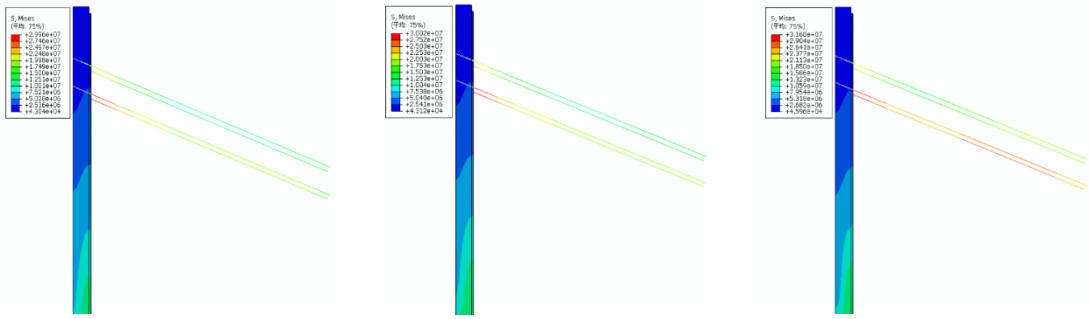

(d) Blockage 60% (e) Blockage 80% (f)Blockage 100%

Fig. 13: Axial force cloud chart of anchor cable

The results show that the change law of anchor rod and axial force with different blocking degree. From the figure, when the blockage degree is less than 80%, the blockage force is greater than 80%, the axial force increases with 60% and 80% and more than 80%, the axial force increases by about 10% compared with the blockage degree of 80%

5.3. Comparison and Analysis of Side Slope Stability

Due to the blockage of the discharge hole, the rock soil tends to saturation state, its shear degree decay to a certain extent, strength subtraction is a reasonable way to calculate the slope stability state, the cohesive force of the rock body and Mocha angle are simultaneously reduced after numerical calculation. $c^{'}$ and $\varphi^{'}$ are the reduced rock mass adhesion and friction angle, respectively, and the calculation model is as follows:

$$\begin{cases} c^{'} = \dfrac{c}{F_s} \\ \tan\varphi^{'} = \dfrac{\tan\varphi}{F_s} \end{cases} \tag{11}$$

In formula (11), Fs is the reduction coefficient of reaching the ultimate equilibrium state, that is, the safety factor. In the numerical calculation, the reduction coefficient of defining the mutation of the characteristic point displacement is the safety factor.

The safety factor of slope is calculated and the relationship between blockage degree and slope safety is studied.In the calculation, the displacement change of a slope top node is the standard. When the slope node displacement changes, the corresponding strength reduction coefficient is the safety coefficient of the slope, and the slope safety coefficient of the two forms of support under different blocking degrees is drawn as a curve as shown in Figure 16.

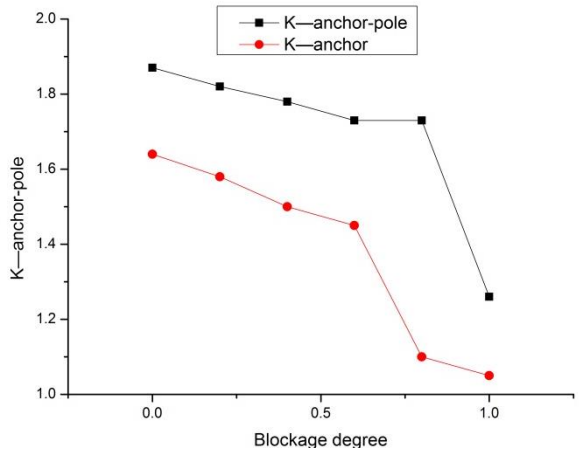

Fig. 14: Variation law of slope safety factor under different degree of blockage

Analysis shows from Figure 14:

ISSN 2706-655X Vol.3, Issue 5: 17-29, DOI: 10.25236/IJFET.2021.030503

(1) In different blockage degrees, the slope safety coefficient of anchor pull pile support is higher than that of lattice anchor rod support. With the increase of blockage degree of drainage hole, the safety coefficient of the slope under the two supporting forms is gradually reduced, and the blockage degree is less than 60%.

(2) When the blockage degree of the drainage hole is greater than 60% and less than 80%, the stability coefficient of both slopes decreases sharply.

6. Conclusion

The influence of drain hole blockage on slope stability by sensor in situ test technology, non-contact near-field photogrammetry technology, numerical simulation method and finite element strength reduction theory were studied, and the following conclusions were obtained:

(1) Monitoring the groundwater by water level meter and pore pressure meter, when the drainage hole blockage exceeds 80%, the pore water pressure of the slope groundwater level increases by about 13m, by 25kPa; by the bar gauge and anchor shaft gauge. When the drainage hole blockage exceeds 80%, the shear force of the slope anti-skid pile increases by 20% and the anchor shaft force increases by about 30kN;.

(2) The slope table deformation is analyzed through near-view photography, when the blockage degree of drainage hole exceeds 80%, the slope deformation of 44mm, exceeds the slope deformation warning value of 30mm,.

3) analyzes the mechanical response of the groundwater level of the slope, and the numerical simulation results show that when the drainage hole blockage degree is less than 60% and the support structure and slope deformation increase linearly, when the blockage degree exceeds 80%, the support structure increases sharply and the blockage degree exceeds 60% and the slope stability coefficient exceeds 60%.Theoretical calculation, numerical simulation calculation and test results analysis are basically consistent.

Description

Research Fund for high-level talents of Guizhou Institute of technology, disturbed earth pressure theory and slope stability research based on disturbed earth pressure theory.

References

[1] Quan Cao, Qingming Li, Wei Xiang , etc.Study on automatic monitoring of foundation pit excavation on adjacent existing subway tunnels [J].Geotechnical Journal, 2012,34 (S1): 552-556.
[2] Jiachun Li .Method and index of rainfall disaster evaluation on road slope [D].Changan University, 2005.
[3]Runqiu Huang.Dynamic process and stability control of rock high slope development [J].Journal of Rock mechanics and Engineering, 2008, (08): 1525-1544.
[4] PFDESCOLL A，CORZO A，ALVAREZ E, et al.The effect of primary treatment and flow regime on clogging development in horizontal subsurface flow constrected wetlands:An experimental evaluation[J].Water research, 2011,45(12):3579-3589.
[5] HUA G F, ZENG Y T，ZHOU Z W, et al. Applying a resting operation to alleviate bioclogging in vertical flow constructed wetlands:An experimental lab evaluation[J].Journal of Environmental Management, 2014,136(8):47-53.
[6] MORVANNOU A，FORQUET N, VANCLOOSTER M, et al. Characterizing hydraulic properties of filter material of a vertical flow constructed wetland[J].Ecological Engineering, 2013,60:325-335.
[7] Zhuo Zhou.Research on mechanism and suggestion of tunnel drainage pipe by groundwater seepage in karst areas [D].Changan University, 2015.
[8] LI Y K，LlU Y Z, Ll G B, et al.Surface topographic characteristics of suspended particulates in reclaimed wastewater and effects on clogging in labyrinth drip irrigation emitters[J].Irrigation Scicncc,2012,30(1):43-56.
[9] Yanfang Liu, Pute Wu, Derlan Zhu, etc.Effect of hardness of drip irrigation conditions on drip blockage [J].Journal of Agricultural Engineering, 2015, (20): 95-100.

ISSN 2706-655X Vol.3, Issue 5: 17-29, DOI: 10.25236/IJFET.2021.030503

[10] Richardson J L, Vepraskas M J.Wetland soil: genesis,hydrology, landscapes and classification [M].Boca Raton, FL: C R C Press, 2000
[11] A.CASELLES - Osorio, J.Garcia.Effect of physico - chemical pretreatment on the removal efficiency of horizontal subsurface - flow constructed wetlands [J].Environ.Polltu, 2007, 145:55 - 63
[12] Wang Enzhi , Hongtao Wang, Xudong Deng."Pipe replacing hole" -drainage hole simulation method [J].Journal of Rock mechanics and Engineering, 2001,03:346-349.